

SUPPLEMENTARY DATA

Catalytic transfer hydrogenation of maleic acid with stoichiometric amounts of formic acid in aqueous phase: paving the way for a more sustainable succinic acid production.

M. López Granados^{*a}, J. Moreno^b, A.C. Alba-Rubio^c, J. Iglesias^b, D. Martín Alonso^{d,e} and R. Mariscal^a

^a *EQS Group (Sustainable Energy and Chemistry Group), Institute of Catalysis and Petrochemistry (CSIC), C/ Marie Curie, 2, 28049 Madrid (Spain)*

^b *Chemical & Environmental Engineering Group, Universidad Rey Juan Carlos, C/ Tulipan, s/n, Mostoles, Madrid 28933, Spain*

^c *Department of Chemical Engineering, University of Toledo, Toledo, OH 43606, United States*

^d *Glucan Biorenewables LLC, Madison, WI 53719, USA.*

^e *Department of Chemical and Biological Engineering, University of Wisconsin-Madison, 1415 Engineering Drive, Madison, WI 53706, USA*

**corresponding author: mlgranados@icp.csic.es*

Preparation of gold supported on carbon catalyst.

Au supported on carbon was prepared by deposition-precipitation. Approximately 0.16 g of the gold precursor ($\text{HAuCl}_4 \cdot 3\text{H}_2\text{O}$, Sigma-Aldrich) was weighed and added to 400 mL of water under agitation. The pH of the gold solution was adjusted to 9 by dropwise addition of a 2.5 M solution of ammonium hydroxide. Then 1.5 g of the support was incorporated, and the pH adjusted again. The mixture was aged and stirred vigorously for 6 hours. The solution was then filtered and rinsed with water to remove the chloride ions out. The recovered solid was dried overnight at room temperature. This precursor was reduced with hydrogen gas for 4 hours at 350°C at a heating rate of 0.5 °C·min⁻¹. After cooling it down to room temperature, the catalyst was passivated with 1% O₂/Ar for 30 minutes.

Preparation of supported Pd catalysts.

Supported Pd catalysts were prepared by incipient wetness impregnation. The support was incorporated to a flask containing the required amount of a solution of the Pd precursor (ammonium tetrachloropalladate (II)). A small portion of the support was initially incorporated to the solution and stirred in order to have a homogeneous slurry before proceeding with further incorporation of the support. Once all the support was

incorporated and homogenized, the solid was dried for 12 h at 120 °C (heating ramp 1.5 °C·min⁻¹) and subsequently calcined at 500 °C (heating ramp 1.5 °C·min⁻¹) under ambient air.

Before conducting the reaction, the catalysts were reduced under 50 mL min⁻¹ of 10 vol.% H₂/Ar flow at 200°C for 2h (heating ramp 1.5 °C·min⁻¹) and then cooled down to room temperature. The reduced catalyst was passivated at room temperature with 200 mL min⁻¹ of 1.5 vol.% O₂/Ar overnight and then transferred from the reduction equipment to the reactor where the catalytic reaction was conducted.

CeO₂, TiO₂, CeZrO₄, WO₃, ZrO₂, Al₂O₃, Silica fumed were purchased from Sigma Aldrich. Titanium silicalite 1 (TS-1) was purchased from ACS Materials. Nicanite support was prepared as described elsewhere [1].

Determination of the amount of CO chemisorbed on Pd particles

The amount of CO chemisorbed over Pd particles was measured by the breakthrough curves obtained by switching the feed passing through the samples from 45 ml·min⁻¹ Ar to a flow containing 45 ml·min⁻¹ Ar and 5 ml·min⁻¹ of a 5v/v% CO/He mixture (equivalent to 0.186 μmol CO·s⁻¹). Helium was used as a trace to set time = 0 for the breakthrough curves (see Figure ESI1 below). Two cycles were conducted, in the first cycle the CO breakthrough curve is delayed with respect to t=0 due to dead volume of the reactor and the irreversible and reversible CO chemisorption (broken line in Fig. ESI1 indicates the hypothetical trace of CO without any chemisorption, shifted only because of the dead volume of the reactor). Once the CO signal reaches a steady value (ca. 20 min.), the feed switches back to only Ar. A second cycle was done once CO is fully removed from the flow and no CO signal is detected (ca. 30 min). The second CO breakthrough curve is delayed because of the dead volume and the reversible CO chemisorption only. The difference between these two breakthrough curves is the irreversible CO chemisorption.

Before the chemisorption, the sample (50 mg) was pretreated first by an oxidation treatment and then by a reduction treatment in order to make sure that the surface of Pd particles was clean of C contamination and fully reduced. The oxidation treatment consisted of heating the sample at 150 °C (heating ramp 5 °C·min⁻¹) for 30 min. under 100 mL/min of 3%O₂/Ar and then cooled down to 30 °C. Subsequently the sample was subjected to a reduction treatment with 50 mL/min of 10% H₂/Ar at 150 °C (heating ramp 5°C·min⁻¹) for 1 h. Then the feed was switched to 100 mL/min of Ar to remove any

chemisorbed H_2 at $150\text{ }^\circ\text{C}$ for 30 min. Once the cleaning procedure is over, the

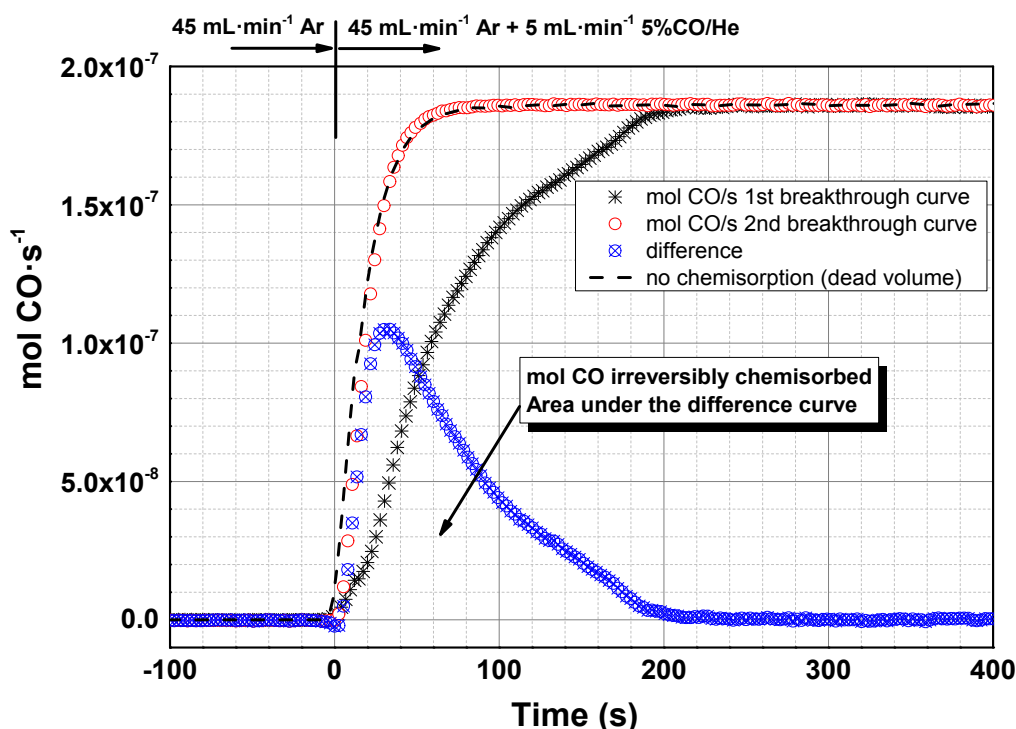


Figure SD-1. Chemisorption of CO by using two consecutive CO breakthrough curves (broken line indicates the hypothetic trace of CO without any chemisorption shifted only because of the dead volume of the reactor).

temperature was reduced to $30\text{ }^\circ\text{C}$ and the chemisorption experiment was conducted. Once the chemisorption experiments were completed, the sample was again pretreated with the oxidizing and the reducing experiments described above, and new chemisorption experiments were conducted. The result tabulated in Table 5 of the main article was the average of three measurements.

Comparison of CTH experiments with MAc, FumAc and both MAc and FumAc

In order to see if the presence of MAc inhibits the CTH hydrogenation of FumAc, the reaction rates when only FumAc was used as substrate (column 2 of Table SD-1) and those obtained when both FumAc and MAc (column 3 of Table SD-1) were measured. For contrasting purposes the rates with MAc is also incorporated in the Table SD-1 (column 1). In the 3rd column case, the sum of both FumAc and FAc concentrations loaded in the reactor equals that of FumAc or MAc in experiments for column 1 and 2. The reactions were conducted under the conditions indicated in the Table. Once the reaction is stopped and the reactor was at room temperature, and after the addition of the internal standard (levulinic acid), few tenths of grams of a 50 % wt. NaOH solution was added to neutralised all the acids with the intention of solubilising FumAc as disodium fumarate. Thus, all FumAc can be analysed by HPLC and FumAc reaction rates can be accurately determined. Actually for this experiments this NaOH protocol allows to reach a carbon balance of 100 % \pm 5 %. The error in reaction rates has been determined to be 1-3 % of the nominal value. The error indicated in the Tables are the consequence of rounding up of a 3 % error in the tabulated values.

Table SD-1. Reaction rates for FAc, FumAc and MAc conversion and SAc formation in Pd/C catalyst, depending on the substrate present in the reactor (reactions conducted in Ace glass reactors). Reaction conditions: 5.7 g of reaction mixture, 0.8 wt. % of catalyst, mol FAc/MAc = 1.1, 110 °C, initial N₂ pressure = 1 bar, and time of reaction 4 h.

Rate mmol/g _{cat} ·min	5 wt.% MAc	5 wt.% FumAc	2.5 wt.% FumAc 2.5 wt.% MAc
-r_{FAc}^a	0.08 \pm 0.00 ₁	0.22 \pm 0.01	0.12 \pm 0.00 ₄
-r_{MAc}^a	0.12 \pm 0.00 ₃	-	0.08 \pm 0.00 ₂
-r_{FumAc}^a	-	0.21 \pm 0.01	0.02 \pm 0.00 ₁
r_{FumAc}^b	0.05 \pm 0.00 ₂	-	-
r_{SAc}^b	0.07 \pm 0.00 ₂	0.22 \pm 0.01	0.09 \pm 0.00 ₃

^a reaction rates of consumption

^b reaction rates of formation

The values of reaction rates correspond to integral rates and not to differential rates because the conversion of MAc/FumAc/FAC and yield of SAc are well above 10 % (for instance, the MAc or FumAc conversion for columns 1 and 2 experiments are 55 and 100 % and in the case of third column the conversions for MAc and FumAc were 69 and 17 %, respectively). Despite of this, the conclusions that are going to be explained are still valid.

The r_{SAc} (rate of formation of SAc) in the first column ($0.07 \text{ mmol/g}_{\text{cat}} \cdot \text{min}^{-1}$) is three times slower than that from FumAc (second column, $0.22 \text{ mmol/g}_{\text{cat}} \cdot \text{min}^{-1}$). The same occurs for the rate of consumption of FAC ($-r_{\text{FAC}}$). For column 1 experiment a small fraction of FAC is decomposed without forming SAc whereas for column 2 all FAC is converted to SAc. These data indicate that FumAc is rapidly hydrogenated to SAc and actually is a better substrate to produce faster SAc via CTH.

Interestingly, for the experiment of column 3, the $-r_{\text{FAC}}$ and r_{SAc} are ca. two times slower than these of column 2, although still faster than that of column 1. Besides, $-r_{\text{FumAc}}$ in the third column is only $0.02 \text{ mmol/g}_{\text{cat}} \cdot \text{min}^{-1}$, ten times slower than in column 2 ($0.22 \text{ mmol/g}_{\text{cat}} \cdot \text{min}^{-1}$). These data demonstrate that CTH of FumAc is seriously inhibited by the presence of MAc. Actually in the experiments of column 3 (when both MAc and FumAc are initially present) SAc is essentially coming from MAc and only a fraction is coming from FumAc, despite of the fact that CTH of FumAc can be three times faster than that from MAc.

Comparison of the catalytic properties of Pd/ C catalyst with other Pd supported catalysts in batch reactors.

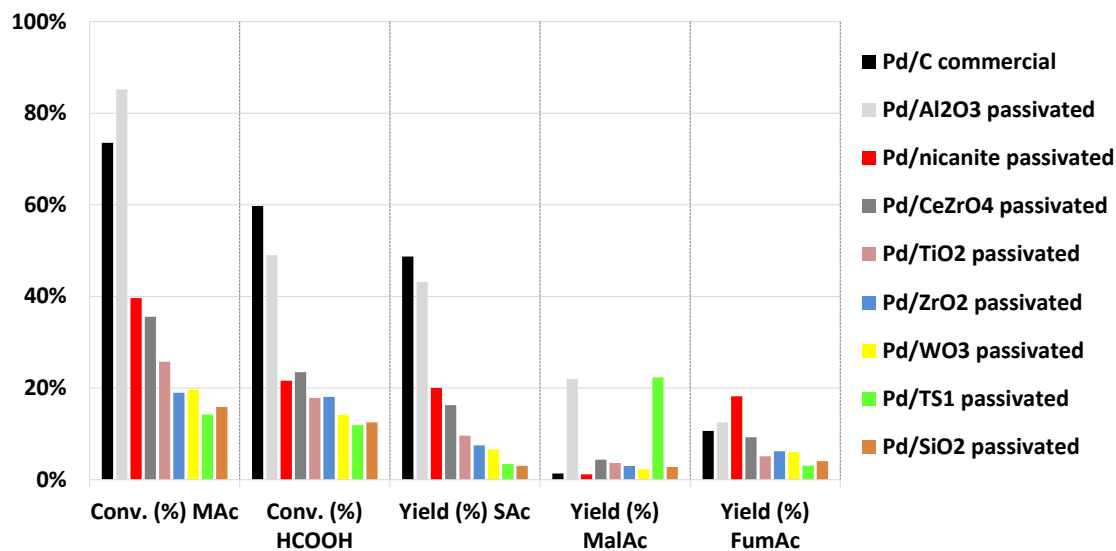


Figure SD-2: Catalytic properties of supported Pd catalysts in batch reactors. Reaction conditions: conc. of MAC solution = 5 wt.%, mol FAc/MAC = 1, 110 °C, 10 bar, 4 h.

Values of pH before and after the reaction

The pH of the reaction mixtures, before and after the reaction, was measured in three different reaction mixtures: MAc and FAc, MAc and sodium formate and finally, reacting disodium maleate with sodium formate. The second case is an intermediate case between the two extreme cases: no neutralisation and full neutralisation of acid protons. The reaction conditions of the catalytic tests and the initial and final pH are those indicated in Table SD-2. These experiments have been conducted with more diluted concentrations than those used in Fig. 4 of the manuscript. Therefore, pH value is a direct measurement of the H^+ and OH^- concentrations and also to prevent the precipitation of maleates and succinates. The conversion of reactants is also close to full conversion, but in any case, the experiments still provide qualitative information of the pH changes taking place under reaction and also of the final pH expected in the experiments conducted in Fig. 4.

Table SD-2. Initial and final pH in three different situations. Reaction conditions: 5 g of reaction mixture conc. of MAc solution = 5 wt.%, wt. catalyst/MAc = 0.2, mol FAc/MAc = 1, 150 °C, 10 bar, reaction time = 2 h.

Reaction conducted with	Initial pH	Final pH
MAc and FAc	1.2	2.1
MAc and sodium formate	2.6	4.6
disodium maleate and sodium formate	12.5	8.9

When the reaction is conducted with the acids (non-neutralised), pH shifts from 1.2 to 2.1, this decrease is consistent with the fact that SAc is a weaker acid than MAc and that formic acid is consumed. The CO_2 gas is released and pressure builds up. When using MAc and sodium formate, the initial pH is 2.6 and shifts to 4.6 once the reaction is completed. The final OH^- concentration is more than two orders of magnitude larger than in the previous case. It is worth recalling that when formate was present in Fig. 4 the reaction rate increases but not two orders of magnitude. There is no direct correlation between the rate and concentration of OH^- . At the other extreme, when formate and maleate are reacted, the initial pH is basic and shifts to lower pH once the reaction is completed (from 12.5 to 8.9) because the released CO_2 neutralises the OH^- anions, forming bicarbonate anion.

Long term catalytic properties of Pd/ γ -Al₂O₃ catalyst under continuous operation in a fixed bed reactor.

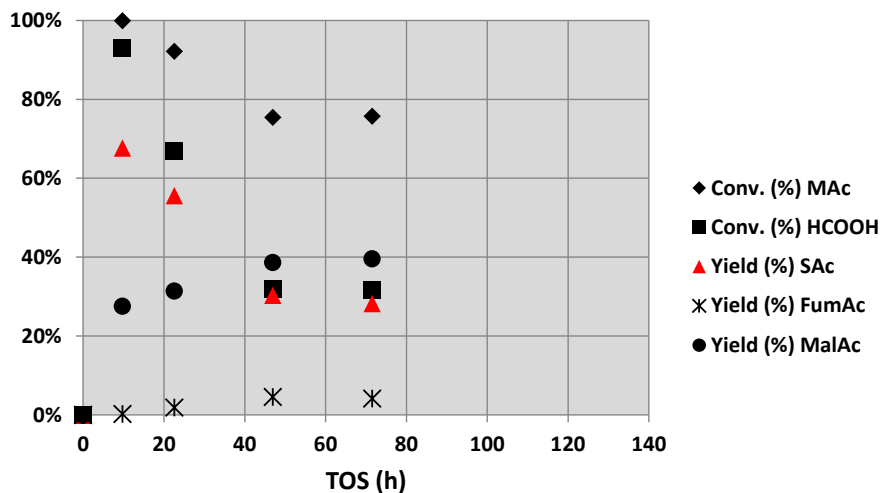


Figure SD-3: Catalytic properties of Pd/ γ -Al₂O₃ catalyst under continuous operation. Reaction conditions: conc. of MAc solution = 2.5 wt.%, mol FAc/MAC = 1, 150 °C, 10 bar, catalyst loading = 0.50 g, WHSV = 12 h⁻¹.

Long term catalytic properties of Au/C catalyst under continuous operation in a fixed bed reactor.

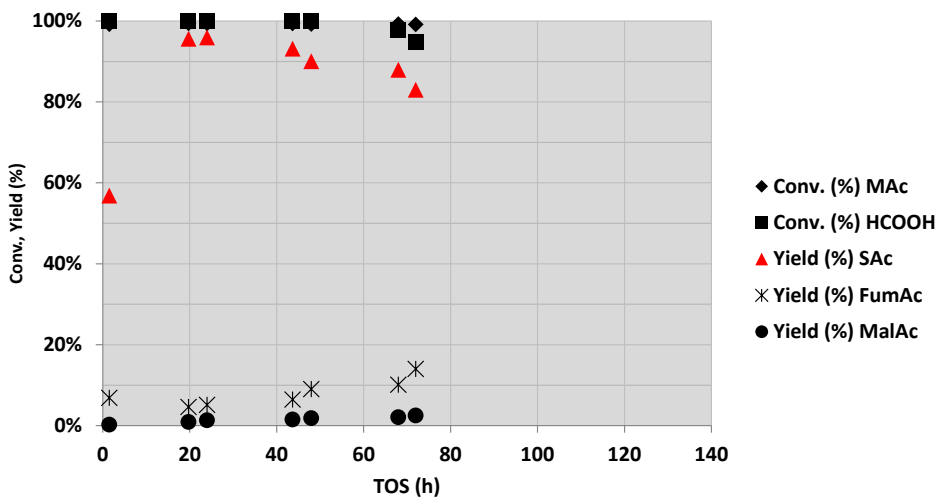


Figure SD-4: Catalytic properties of Au/C catalyst under continuous operation. Reaction conditions: conc. of MAc solution = 2.5 wt.%, mol FAc/MAC = 1, 150 °C, 10 bar, catalyst loading = 0.50 g, WHSV = 12 h⁻¹.

TEM results

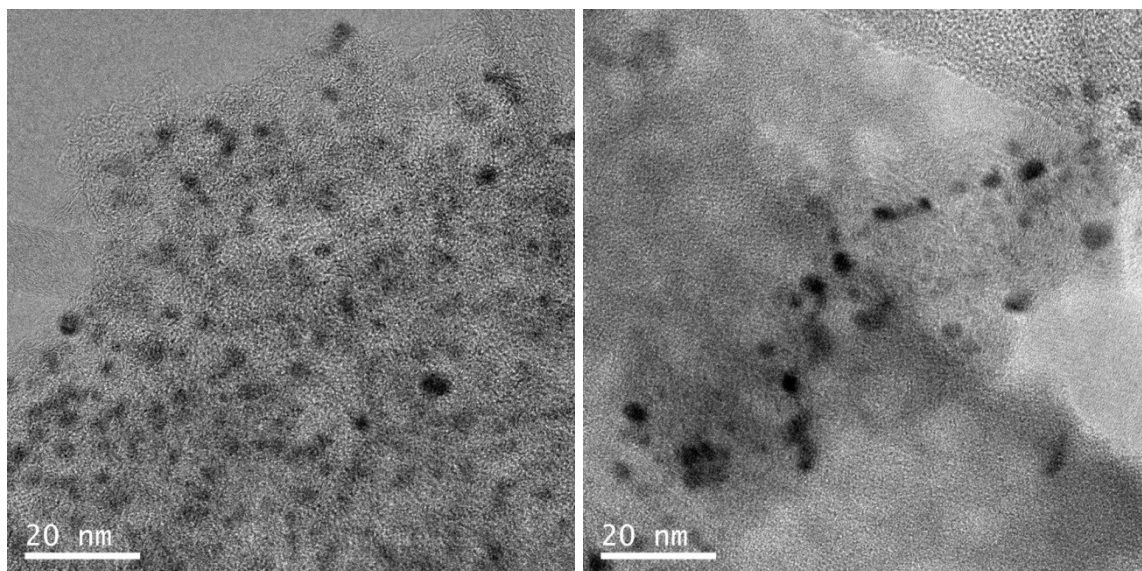


Figure SD-5. Representative TEM pictures of fresh (left) and used (right) commercial Pd/C, the latter corresponds to that of Fig. 4 of the main article

Catalytic results in batch reactors using gas H₂

The catalytic properties using gas phase H₂ were also examined. First, it was observed that when formic acid is fully decomposed to H₂ and CO₂ in the absence of MAc and under the same conditions of Figure 1, the pressure built-up in the reactor at room temperature was quite close to 4 bar, what implies that the partial pressure of H₂ supplied by FAc decomposition is 2 bar (the rest coming from CO₂). When the MAc is reacted with 2 bar of gas H₂ in the absence of FAc (the rest of reaction conditions are those of Figure 1), the yield of SAc after 2 h of reaction was close to 60 %. In contrast, when formic acid was used the yield obtained was 77.0% (Figure 1). Then the result of Fig. SD-6 represents the 78 % of the value obtained with FAc. Moreover, it must be stressed that the theoretical contribution of the H₂ released from the decomposition of formic acid must be much smaller. In the experiments with gas phase H₂, the latter is available from the very beginning whereas in experiments with FAc (that of Figure 1) the initial pressure of the hypothetical H₂ released from FAc decomposition would be zero and build-up as decomposition proceeded (assuming that there is no CTH contribution). Consequently, the contribution of the gas phase H₂ route to the overall reaction is smaller than that

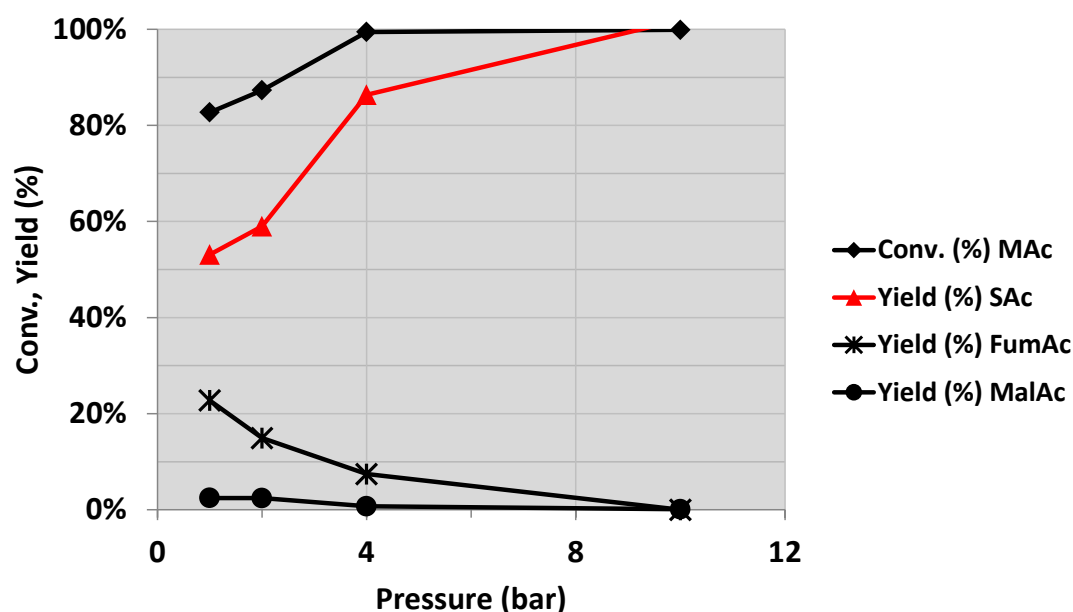
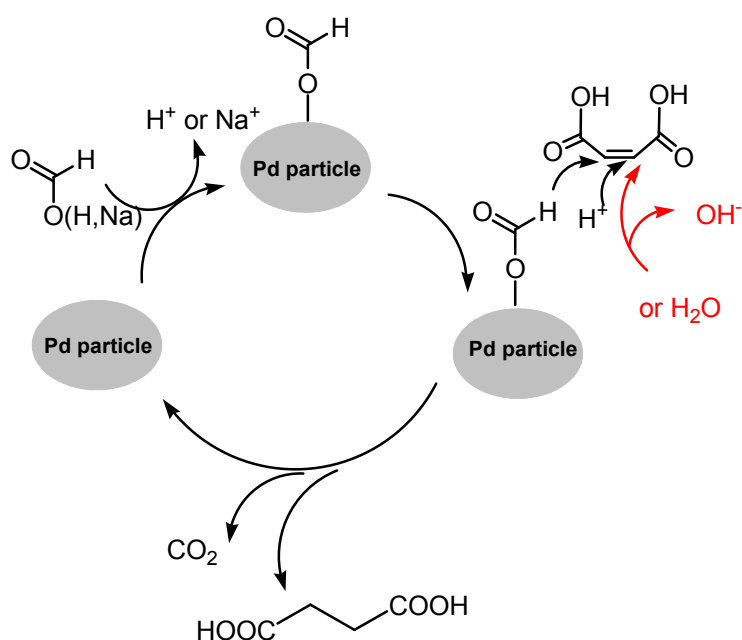


Figure SD-6: Effect of pressure on the catalytic properties. Reaction conditions: 5 g of reaction mixture, 5 wt.% MAc, 1 wt. % of catalyst, mol FAc/MAc = 1, 150 °C, reaction time = 2 h, initial N₂ pressure = 10 bar.

suggested from the raw data of Fig. SD-6. This suggest that, at the very least, CTH route is involved in the reaction with FAc.

Scheme of the proposed CTH mechanism

We proposed the concerted intermolecular CTH mechanism depicted in Scheme 1. For the sake of clarity in the scheme an Eley-Rideal mechanism was assumed, i.e. adsorbed formate reacts with non-adsorbed MAc; but MA, protons or H₂O species can also be adsorbed on the Pd surface. Formic acid is chemisorbed as formate and the acid H⁺ is released (H₃O⁺ is actually present in the aqueous solution). Next step is the concerted attack of the formyl H of adsorbed formate (indicated by an arrow) and another H to the C=C bond (also indicated by an arrow). The latter can come either from acid protons in acidic pH or from water in neutral pH (in red in Scheme SD-1). With the information gathered so far it is not completely clear which is responsible for the donation. In the case of using fully neutralized maleate and formate, H₂O supplies the second H releasing OH⁻ that electrically compensates the Na⁺ cations (represented in red in the scheme). In this latter case the reaction proceeds much faster than in acidic pH.

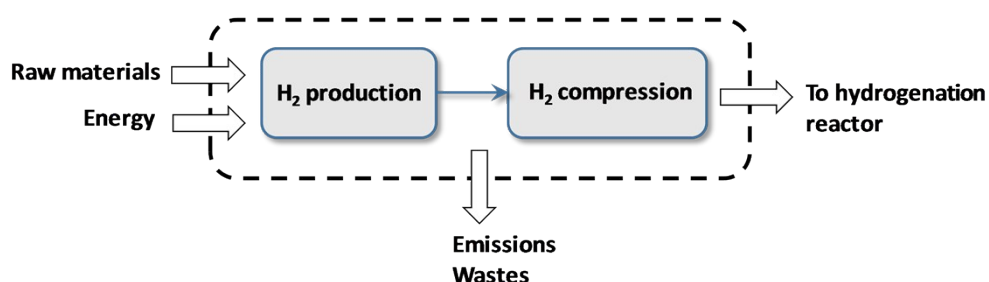


Scheme SD-1

Procedure for preliminary LCA calculations

Figure SD-7 displays the boundaries of the evaluated systems. We have only included the production of the reduction agents (H_2 or FAc) as well as the compression of a hydrogen stream up to the reaction pressure. This approach considers the use of different reagents and operation conditions in both alternatives. Additionally, the direct CO_2 emissions coming from formic acid decomposition were also considered for the FAc system.

SYSTEM 1: H_2 AS REDUCTION AGENT (CONVENTIONAL HYDROGENATION)



SYSTEM 2: FORMIC ACID (FAc) AS REDUCTION AGENT (CATALYTIC TRANSFER HYDROGENATION)

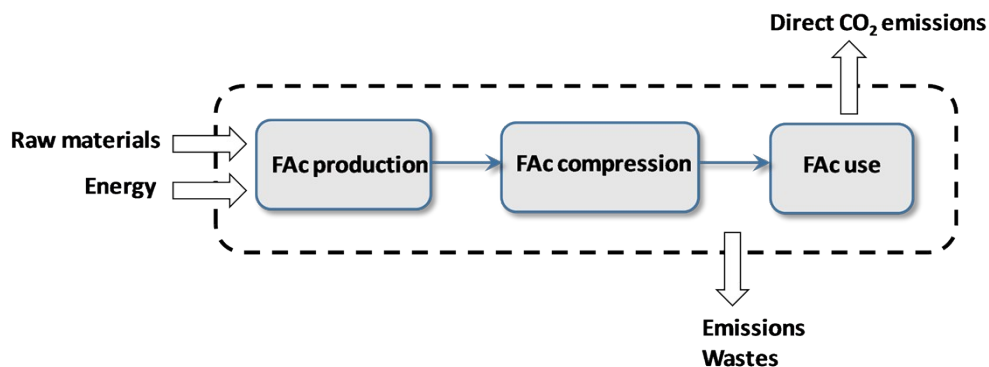


Figure SD-7: Boundaries of the simplified evaluated systems.

For high-pressure hydrogen (system 1), it was assumed that the production of 1 kg of SAc requires 0.254 kg of H_2 compressed at 4.0 MPa according to the work of Pinazo et al. [2]. This amount of H_2 is produced by steam reforming of gas natural (the most usual industrial process [3]) and the necessary pressure is reached by a polytropic compression that consumes 2.5 MJ of electricity. To estimate the environmental impacts caused by the electricity generation, the European power mix of 2018 reported by Jones et al. [4] was considered. Table SD1 displays the contribution of each energy source to this European power mix. Regarding to the system based on the catalytic hydrogen transfer with FAc

(system 2), it was assumed the continuous operation conditions reported here (mol FAc/MAc = 1, 150 °C, 10 bar -1MPa-), leads to a SAc yield close to 98 %. That means the production of 1 kg of SAc requires 0.40 kg of FAc that must be compressed up to 1 MPa. Within this pathway, formic acid was assumed to be produced by hydrolysis of methyl formate, the most extended industrial process [5]. Finally, calculation of electricity consumption of the pump for FAc impulsion evidenced the negligible contribution of this step.

Table SD-3. Power electricity mix of EU (year 2018) [4]

Fuel Type	Share (%)
Lignite	9.2
Hard coal	10.0
Other fossil	4.0
Gas	18.9
Nuclear	25.5
Hydro	10.6
Solar	3.9
Wind	11.8
Biomass	6.1

Two LCA databases (GaBi database and Ecoinvent V2.2) were used for completing systems information. Thus, steam reforming of gas natural was considered from GaBi database: process called “*steam reforming - natural gas, production mix, at producer, DE*”, a data set corresponding to the technologies and specific characteristics of the production of hydrogen in Germany. On the other hand, information for formic acid production was taken from Ecoinvent database: process called “*formic acid from methyl formate, at plant, RER*”, which is modelled according to production data of this chemical in Europe.

Environmental impact quantification was calculated by using the LCA software GaBi 6.0. The following impacts categories were selected and calculated according to the International Reference Life Cycle Data System (ILCD handbook) [6] climate change (CC, measured as kg CO₂-eq.), resource depletion (RD, fossil and mineral, measured as kg Sb-eq), total human toxicity (HT, cancer + non-cancer, measured as comparative toxic

units for humans, CTUh) and photochemical ozone formation (POF, measured as kg of non-methane volatile organic compounds, kg of NMVOC-eq). Besides, the consumption of total freshwater (kg water) and the cumulative energy demand, (CED, measured as MJ-eq) Nuewere also included for systems comparison.

Details of LCA results

Table SD-4. Values of the environmental impacts indicators and percentage contribution of the different steps (referred to 1 kg of SAc).

Impact category	Conventional hydrogenation (with H ₂)			Catalytic hydrogen transfer (with FAc)		
	Mid-point value	H ₂ product. (share %)	Electricity consumpt. (share %)	Mid-point value	FAc product. (share %)	Direct CO ₂ emissions (share %)
Climate Change (kg CO ₂ -eq)	3.0	91.1	8.9	1.6	76.2	23.8
Resource Depletion (kg Sb-eq)	1.2·10 ⁻⁵	41.1	58.9	1.0·10 ⁻⁵	100	0
Total freshwater (kg)	0.45	52.0	48.0	0.38	100	0
Human toxicity (CHTh total)	1.0·10 ⁻⁷	4.2	95.8	2.9·10 ⁻⁷	100	0
Photochem. O ₃ formation (Kg NMVOC)	2.3·10 ⁻³	71.5	28.5	2.8·10 ⁻³	100	0
Cumulative energy demand, CED (MJ)	62.1	88.0	12.0	29.1	100	0.0

References

- [1] F. Fina, S.K. Callear, G.M. Carins, J.T.S. Irvine, Structural investigation of graphitic carbon nitride via XRD and neutron diffraction, *Chem. Mater.* 27 (2015) 2612–2618. <https://doi.org/10.1021/acs.chemmater.5b00411>.
- [2] J.M. Pinazo, M.E. Domine, V. Parvulescu, F. Petru, Sustainability metrics for succinic acid production: A comparison between biomass-based and petrochemical routes, *Catal. Today.* 239 (2015) 17–24. <https://doi.org/10.1016/j.cattod.2014.05.035>.
- [3] P. Nikolaidis, A. Poullikkas, A comparative overview of hydrogen production processes, *Renew. Sustain. Energy Rev.* 67 (2017) 597–611. <https://doi.org/10.1016/j.rser.2016.09.044>.

- [4] D. Jones, A. Sakhel, M. Buck, P. Graichen, The European Power Sector in 2018: up to date analysis on the enrgy transition, (2019).
- [5] J. Hietala, A. Vuori, P. Johnsson, I. Pollari, W. Reutemann, H. Kieczka, Formic acid Formic acid, Ullmann's Encycl. Ind. Chem. (2016).
https://doi.org/10.1002/14356007.a12_013.pub3.
- [6] ILCD Handbook. Recommendations for Life Cycle Impact Assessment in the European context. JRC European Commission., 2011.
<https://doi.org/10.1017/CBO9781107415324.004>.